Contrib Mineral Petrol (1988) 99:176–185

Contributions to Mineralogy and Petrology

Cations in olivine, Part 1: Calcium partitioning and calcium-magnesium distribution between olivines and coexisting melts, with petrologic applications

Amy J.G. Jurewicz* and E. Bruce Watson
Department of Geology, Rensselaer Polytechnic Institute, Troy, New York 12180-3590, USA

Abstract. As part of a study of kinetic and equilibrium aspects of magmatic olivines (Jurewicz 1986; Jurewicz and Watson 1988), calcium distribution and partitioning systematics have been experimentally determined for olivine/melt pairs under a wide variety of temperatures, pressures and oxygen fugacities.

The calcium content of an equilibrated olivine depends upon (1) the concentration of calcium in the melt and (2) the relative activity of iron as indicated by the fayalite content of the olivine. Neither oxygen fugacity nor temperature directly affects the calcium content.

To quantify the influence of iron activity, the partition coefficients for calcium were compiled for selected olivine/melt pairs. This compilation represented systems having a variety of iron activities (olivines of 55% to 96% molar forsterite) and a restricted range of calcium activity (melts having less than 8% to 15% CaO, by weight). The empirical relationship describing the effect of iron is

$$K_d = 0.01\ \{(-0.08 \pm 0.015)\ (\%fo) + (9.5 \pm 0.2)\} \quad (1)$$

where K_d is the experimentally-determined partition coefficient for calcium (the weight ratio of calcium in the olivine to that in the melt) and $\%fo$ is the molar percentage of forsterite in the equilibrated olivine.

In order to compare the calcium systematics among systems exhibiting different iron activities, the calcium partitioning data was normalized. The empirical normalization used is

$$K_{d90} \approx K_d - 0.0008(\%fo - 90) \quad (2)$$

where K_{d90} represents the weight-ratio partition coefficient of a "standard" olivine containing 90% molar forsterite. Use of K_{d90} eliminated the scatter of partitioning data caused by different iron contents, so that the influences of calcium activity and pressure were constrained.

The "best fit" for the dependence of K_{d90} on the measured CaO content of the melt is

$$K_{d90} = 0.021 \quad (3a)$$

for melts with less than 11% CaO by weight and

$$K_{d90} = 0.001\ \{(2.2)\ (\%CaO_{melt}) - 4.3\} \quad (3b)$$

for melts with between 11% and 22% CaO by weight. By comparing the K_{d90} of field samples with these "best fits", natural systems can be tested for equilibrium with respect to calcium.

The dependence of K_{d90} on pressure was negligible for pressures below 20 kb. At 20 kb and above, the limited experimental data yielded ambiguous results, so no ΔV was calculated. Pressure is, however, not likely to influence calcium partitioning in magmatic systems.

The calcium/magnesium exchange was also investigated and was found to be strongly temperature dependent. To isolate the affect of temperature from that of composition, the calcium content of each olivine was normalized to CaO_{90} (where CaO_{90} equals $(K_{d90}) \times (\%CaO$ in the melt)). The molar CaO_{90}/MgO ratio of the olivines were then plotted versus the molar CaO/MgO ratio for the corresponding melts. The data plot on isothermal lines which can then be used as a geothermometer. Standardized isotherms for this equilibrium are presented in Fig. 6.

In influence of pressure on the calcium/magnesium exchange geothermometer was found to be negligible for systems equilibrated below 20 kb. For samples equilibrated at 20 kb and above, pressure may cause low temperature estimates. Unfortunately, the precision of the compiled experimental data did not warrant the calculation of a ΔV for the exchange.

Introduction

Calcium is an almost universal minor constituent of natural olivines and may be present in concentrations of up to one weight percent CaO (Simkin and Smith 1970). Many workers have speculated that calcium systematics might be useful for interpreting the environment of olivine crystallization, a suggestion based on empirical studies of natural olivines (Sahama and Hytonen 1958; Murata et al. 1965; Simkin and Smith 1970), theoretical models (Stormer 1973) and experimental studies (e.g., Watson 1979). The relevant equilibria have been discussed in both the geologic and materials literatures. Synopses are given in Watson (1979) and Jurewicz (1986).

Despite the numerous studies, the factors that influence calcium partitioning and distribution between olivines and coexisting melts are not well characterized. The studies offer conflicting results for two main reasons. First, some of the

* Currently, a visiting scientist at Air Force Wright Aeronautical Laboratories, (MLLM) Wright-Patterson AFB, OH 45433

Offprint requests to: E.B. Watson

early work has been discredited by failure to achieve equilibrium (Yang 1973; Biggar and O'Hara 1969), expecially in dry systems (Yang 1973). This cast doubt on the ability to equilibrate olivines with respect to calcium during experiments (e.g. Watson 1979; Ford et al. 1983). Second, if the crystals are small, and/or the spot-analyses are performed near a calcium-rich phase, casual electron microprobe analyses of olivines may contain spurious "CaO" contributed by "secondary" or "phase boundary" fluorescence (e.g. Watson 1979; Adams and Bishop 1986). This excess CaO contribution is usually small (less than 0.1% CaO by weight for forsteritic olivines adjacent a glass 13.4% calcium by weight, WDS analyses). Unfortunately, that contribution may be many times the actual concentration of CaO in olivine. Accordingly, the large data base available for the study of calcium in magmatic olivines contains hidden errors that can obscure the actual trends.

The recognition of problems with analyses and achieving equilibrium has biased conclusions of previous workers. For example, Ford et al. (1983) saw that previous workers found calcium partitioning to be apparently independent of composition (Simkin and Smith 1970; Watson 1979) and recognized that they could have problems with their compiled data. Therefore, they attributed scatter in their plots of compiled calcium data to analytical difficulties or problems attaining equilibrium. The results of this study suggest that much of that scatter may have been caused by differences in iron content.

Watson (1979) is the only experimental study of calcium partitioning between olivines and basalt-like melts in which a good case is made for both equilibrium and the absence of secondary fluorescence effects. The work demonstrated that: (1) the CaO content of forsterite is linearly dependent on the concentration of calcium in the melt (at low calcium contents), but is indepndent of temperature; and (2) the molar calcium/magnesium distribution coefficient (the ratio of CaO to MgO in the forsterite to that in the melt) depends strongly on temperature. Moreover, both the partitioning and distribution systematics seemed to be independent of the composition of the melt. Accordingly, Watson (1979) suggested that calcium in olivine might be calibrated as a geothermometer. However, the results were not directly applicable to natural compositions because the system used was iron-free and the experiments were all at one atmosphere pressure.

This study extends the experiments of Watson (1979) to ironbearing systems. Data found in the literature are included, so that the compositions used span the range of bulk compositions likely to be found in terrestrial systems (Roeder 1974), as well as some lunar compositions (Delano 1980; Longhi et al. 1978). This compiled data was, however, edited to exclude studies where (1) equilibrium may not have been attained or (2) secondary fluorescence may have influenced analyses. The effects of temperature, pressure, composition and oxygen fugacity on calcium equilibria are examined and the CaO/MgO distribution is calibrated for use as a geothermometer.

Approach to the problem

Experiments were performed both to isolate the effects of temperature, oxygen fugacity, composition and pressure and to demonstrate that samples had equilibrated. Accordingly, two types of experiments were used: (1) crystallization from a melt and (2) reversal of the crystallization by the diffusive exchange of cations (Watson and Green 1981; Watson et al. 1985; Jurewicz and Watson 1988).

The crystallization experiments were performed using relatively standard petrologic techniques. Charges were either pelleted oxide/carbonate mixes or glass beads. These were crystallized using either a controlled atmosphere furnace or a piston-cylinder apparatus (for pressure of up to 25 kb). A diversity of starting materials (natural, doped-natural and synthetic; cf. Table 1) was used for two reasons. First, this wide compositional range allowed the affect of composition to be separated from the influences of temperature, pressure and oxygen fugacity. Second, the variety of compositions allowed a wide range of temperatures and pressures to be attained, while keeping olivine stable with melts that comprised 50% by volume of the charge. This large amount of melt enhanced the mass-transport kinetics and provided a large reservoir of material that remained relatively constant in composition during the experiments. Accordingly, equilibrium was approached rapidly, olivine zoning was avoided, and a stable composition melt was effectively maintained. The constant melt composition was required for the analysis of the reversal experiments described below (details in Jurewicz 1986).

The reversal experiments simply entailed recovering material from a short-duration crystallization experiment, placing it in physical contact with an olivine cube and then running the couple under the appropriate conditions. Accordingly, charges for the reversal experiments were composed of a cube of olivine hung adjacent to a partially crystalline glass bead (the small olivine crystals in the glass were grown under run conditions). Both the source glass and the run conditions were chosen so that they duplicated those of crystallization experiments, so that the results could constitute "reversals" of equilibrium.

A photomicrograph of a post-run charge is given in Figure 1a. The theory for using these runs as reversals is discussed later, in the section Evidence for Olivine/Melt Equilibrium. Charges were also used to determine diffusion parameters for cations in olivine (Jurewicz and Watson, 1988).

Materials and their preparation

The one atmosphere experiments performed to quantify the effects of temperature and oxygen fugacity required that an effectively constant composition olivine be on the liquidus. The compositions used for these experiments are labeled as the MMB-Series in Table 1. For these compositions, the olivines produced were between 89% and 95% molar forsterite for runs between 1200° C and 1350° C, respectively. This system had several other useful properties: (1) olivine was on the liquidus at 1350° C, with no other mineral present until below 1250° C, when either OPX or CPX crystallized (approximately 70% melt, by volume); (2) the iron activity was low, so that iron loss was easy to avoid; and (3) the highly forsteritic olivines were stable over a wide range of oxygen fugacity (e.g. Nitsan, 1974). In addition, the mixes could be considered as analogs for picrites or high-magnesium basalts; i.e., low in alkalis, high in magnesium, and having olivine on the liquidus, followed by orthopyroxene (protoenstatie) and clinopyroxene. However, there was a more than twofold change in the calcium concentration in the melts.

The MMB series compositions were prepared by first combining the oxide, or carbonate, of all the components except calcium. Then 8–20 weight percent CaO was added to separate aliquots of the mix to produce the final, desired compositions. Two batches

were made which, according to later microprobe analyses, differed in one having trace amounts of Na and K; however, this difference did not appear to influence the experimental results.

The MMB-series materials were unsuitable for determining the effect of pressure, because at elevated pressures (a) the liquidus temperature became impractically high, and (b) orthopyroxene replaced olivine as the liquidus mineral (cf. Stolper 1980). Instead, charges for high-pressure crystallization experiments consisted of an oxide/carbonate mix (similar to NT-23 of Elthon and Scarfe 1984), plus a variable fraction of San Carlos olivine. This olivine fraction was added to insure that the melts were saturated in olivine at elevated pressures: the amount of olivine to add was determined by plotting the calculated composition of San Carlos olivine/oxide/carbonate mixes on the triangular phase diagrams of Stolper (1980). Up to 78 weight percent olivine was added to insure the presence of olivine on the liquidus at pressures up to 25 kb; therefore, bulk compositions more closely approximated olivine cumulates than the MORB or MMB-series compositions that were used at one atmosphere.

To understand the role of composition in calcium equilibration, several other compositions were used (also listed in Table 1).

All of the cubes of natural olivine used the diffusional-reversal experiments were of gem-quality, homogeneous St. John's olivine (again, Table 1). The sides of the cubes were 0.75–2 mm in length and usually, but not always, had a well-developed (001) face. Where present, this face was striated parallel to the *c* axis, and was used to orient the cubes both before and after the runs. Those cubes which did not have a well-developed crystal face were polished with ≥ 0.3-micron alumina on at least one side. Compiled results later indicated, however, that even unpolished cut faces often showed usable diffusion profiles (cf., Jurewicz, 1986; Jurewicz and Watson, 1988).

For diffusion (reversal) experiments performed in the controlled atmosphere furnace, the composition used for the melt reservoirs were the same as those used for corresponding crystallization experiments (cf. Jurewicz 1986). The reservoir material for high-pressure diffusion experiments was made from a mixture of 78 weight percent NT-23 and 22 weight percent San Carlos olivine. By necessity, all the mix was melted in a single piston cylinder run at 1500° C and 18 kb and subsequently quenched to form a glass/quench crystal aggregate.

Experimental procedures

A synopsis of procedures for the four types of experiments (crystallization and diffusion, at low and high pressures) is given below. For details, see Jurewicz (1986).

One atmosphere runs

Charges for one-atmosphere experiments were mounted on iron-doped platinum loops using a technique similar to that described in Walker et al. (1979), but different in some important details. For example, newly iron-doped platinum-wire loops were used for each run: the melt (glass) used as a source of iron had been dissolved by soaking the resultant charge in dilute hydrofluoric acid (HF) for 6 hours to overnight, as necessary; residual material was removed both by manual scraping under a binocular microscope and by ultrasonic cleaning. The iron-doping run was not a complete blank experiment, unless the loops were intended to support (a) charges subjected to long, high temperature runs (such as the exchange experiments), or (b) charges containing higher iron contents.

One-atmosphere charges were either pelleted powders, partially crystalline glass beads, or diffusion couples, as described previously. Powders of oxides or natural rocks were mounted on platinum loops by mixing them with acetone and an acetone-soluble hard wax binder (where necessary), using a dental amalgam carrier to pack the mix onto the loops as dense pellets. These pellets were air dried and then briefly fired in an oxygen-natural gas flame. Glass beads were supported using the loop on which they were formed. Olivine cubes for diffusion experiments were supported by a loose, double-loop of undoped 0.005″ platinum wire.

The controlled-atmosphere furnace was brought to run conditions over the course of an hour. The furnace temperature was regulated to $\pm 1°$ C and independently monitored using a Pt/Pt10%Rh thermocouple that was protected from the furnace gas by a closed alumina sheath. The oxygen fugacity (fO_2) in the furnace was controlled by specifying the ratio of carbon monoxide to carbon dioxide in the gas mixture (Deines et al. 1974) and monitored using a yittrium-doped zirconia electrode, as detailed by Arculus and Delano (1981). Experimental charges were directly exposed to the CO/CO_2 furnace gas throughout the run. Total combined gas flow rates ranged from 0.7 to 0.9 cm/s (Darken and Gurry 1945; Sato 1971), with the actual flow rate depending upon the sensitivity of the fO_2 to small fluctuations in the amounts of CO or CO_2 in the mix (Jurewicz 1986). CO/CO_2 ratios were calculated using the equations of Deines et al. (1974), while the oxygen fugacity of any standard buffer used for comparison was determined using the equations of Huebner (1971). The MBASIC program used to calculate run parameters is listed in Jurewicz (1986) and is available from the first author upon request.

High-pressure experiments

Charges for high temperature crystallization experiments consisted of oxide-carbonate-San Carlos olivine mixes packed in graphite capsules. During the run, these powders were first melted at 50–100° C above run conditions to insure the dissolution of all San Carlos olivine and then dropped to the final temperature. Later, the "melt olivines" were inspected, looking for unequilibrated relict olivines. Charges for reversal (cation-exchange) experiments consisted of an oriented cube of St. John's olivine packed in an olivine-saturated glass/quench crystal aggregate (cf. Materials and their preparation).

For all high-pressure experiments, charges were run in a piston-cylinder apparatus using $^1/_2$″ assemblies composed of an outer NaCl sleeve, an inner Pyrex sleeve and base, and crushable Al_2O_3 internal supports. Quenching took place within a few seconds after the power was turned off. Temperatures were measured and controlled using a W3%Re/W25%Re thermocouple with no adjustment for pressure effects on EMF. The piston-in technique was employed, with no friction corrections. Accuracies for the reported temperatures and pressures reported are believed to be within $\pm 15°$ C and ± 1 kb, respectively.

No independent means of monitoring or controlling the ambient oxygen fugacity could be employed. Empirical results from test runs had previously shown the ambient fO_2 in graphite capsules to be near NNO at run conditions; however, because the samples were run dry in graphite capsules, fO_2's were only constrained to be at or below the graphite/CO/CO_2 buffer. In addition, all melts were saturated with graphite.

Determination of compositions

In all of the experiments, the final contents of the charges were olivines coexisting with melts, and sometimes other phases. Olivines and non-volatile glasses were analyzed by wavelength dispersive spectroscopy (WDS) on a Cameca automated microprobe. Standard procedures included a 15 kV accelerating voltage, automatic fixed time or fixed count for specified accuracies, and ZAF corrections (cf. Goldstein et al. 1975). A point beam was used on crystals and alkali-poor glasses, while a round spot up to 100 microns in diameter was used on the more alkali-rich glasses to minimize volatilization of the sample.

The problem of secondary fluorescence (or phase boundary fluorescence; Adams and Bishop, 1986) in the calcium analyses was dealt with in the following manner. First, for each analysis, detailed notes were taken on where the electron beam was situated relative to the glass/crystal interface. Then, during data-reduction, affected analyses were either: (1) dropped, if there were more than four unaffected analyses for that sample, or (2) the affected data

were corrected for their component of secondary fluorescence. Corrections were made by subtracting the appropriate component of a digitized secondary fluorescence profile. The profile had been measured previously on St. John's olivine/melt couple prepared just for this purpose by running a "zero time" experiment (cf., Misener 1974; Watson 1979; Harrison and Watson 1983).

Because of the high sample currents employed, the WDS gave very poor analyses on some of the alkali-rich glasses. Therefore, energy dispersive spectroscopy (EDS) was used on glasses which could not be easily analyzed using WDS techniques. These analyses were performed on the ETEC Autoprobe at The State University of New York at Albany. Routine operating procedures included a 15 kV accelerating voltage, 30 s count times, a minimum of six repetitions per phase, fayalite and quartz standards, and Bence-Albee corrections. As a cross-check, several charges were analyzed on both the Cameca and the ETEC. No significant analytical differences were found for run products of olivine, pyroxene or non-volatile glass.

Further details of analytical procedures are given in Jurewicz (1986).

Evidence for olivine melt equilibrium

Several lines of evidence were used to insure the equilibration of experimental charges, because calcium in olivine was previously found to be difficult to equilibrate (Yang 1973, Ford et al. 1983).

The most definitive evidence comes from the diffusive exchange experiments. The photomicrograph in Fig. 1a illustrates the sample geometry (cf., Approach to the problem, this paper; Jurewicz 1986). Figure 1b shows a diffusion profile formed during a run. In theory, the surface of a foreign olivine equilibrating with a large quantity of melt is converted to the equilibrium composition (Watson and Green 1981; Watson et al. 1985). At the same time, the small unzoned melt olivines (grown during an initial, short-term crystallization experiment) should represent the equilibrium composition. Accordingly, when the partition coefficient for each element measured in the melt olivines agrees with that calculated from the corresponding diffusion profile, a reversal of equilibrium is demonstrated (Watson et al. 1985). The iterative procedure of Watson et al. (1985) was used to determine these partition coefficients. In general, for each element, the calculated and measured olivine agreed, given ± 2 standard deviations for error in each procedure. However, when determining equilibrium, a ± 3-standard deviation leeway was allowed to compensate for the several sources of error not included in counting statistics or curve-fitting (cf., Jurewicz 1986; Jurewicz and Watson 1988; Crank 1975, p 234). Details are given in Jurewicz (1986).

Other evidence also suggested a close approach to equilibrium. Crystals, some over 0.5 mm in diameter, were inspected thoroughly using microprobe traverses and/or backscattered electron imaging and found to be homogeneous. Two samples were run for different times and checked for consistency of results. Olivines were grown in two initially identical charges by crystallization from a glass and a melt, respectively and found to have the same final composition. Finally, Fe/Mg distribution coefficients were calculated for the MMB-series, and only three values were not within 0.30 ± 0.02 (Roeder and Emslie, 1970). These charges all had high Fe/Mg distribution coefficients, and because they were all run below IW it was assumed they suffered iron loss. Accordingly, they were not used in curve fitting. The clear systematics followed by the remaining data, and their consistency with data in the literature also implied that equilibrium was attained.

Results

The effects of temperature and oxygen fugacity. To isolate the effects of temperature and oxygen fugacity on calcium equilibria, runs were performed in which pressure was held at approximately one bar in a controlled-atmosphere furnace and olivine compositions with low iron content were used to keep the activity of iron was nearly constant (cf. Approach to the Problem). Variations in the activity of CaO among charges were found to contribute only a small amount of scatter and did not obscure the results. A summary of derivative olivine and melt composition data and run parameters for this series of experiments is given in Table 2.

The trends in calcium partitioning given in Table 2 are illustrated in Fig. 2a, a plot of the CaO concentration of the olivines versus the CaO concentration of the coexisting liquids, in weight percent (excluding charges showing iron loss). No dependence on temperature or oxygen fugacity is evident. In fact, for olivine coexisting with melts having calcium contents between 9 and 18 weight percent, the data set is nearly linear, with a correlation coefficient, r, of 0.97.

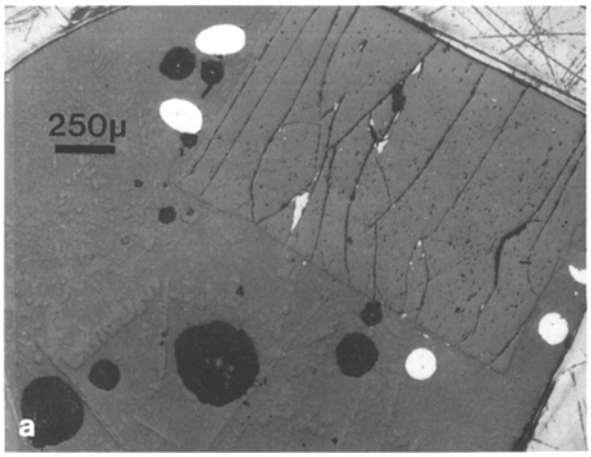

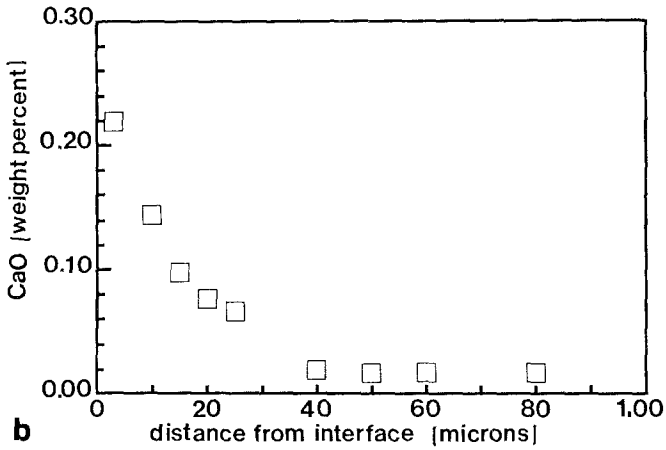

Fig. 1 a, b. A diffusional-exchange experiment run under a CO/CO_2 atmosphere [QFM oxygen buffer ($\sim 10^{-8}$ atm)] at 1200° C, for ten days. **a** Reflected light photomicrograph of the charge. Blade-like crystals are melt olivines; dark spheroids are bubbles; white spheroids are 0.005 inch platium wire. The St. John's olivine shows cleavage-cracking from the quench; **b** CaO (wt%) versus distance from the glass/olivine interface of the St. John's olivine cube (above), parallel to the *a*-crystallographic direction. Calcium values have been corrected for secondary fluorescence. Initial calcium in the St. John's olivine is 0.01% by weight; final calcium in the olivine is calculated to be $0.28\% \pm 0.03\%$ by weight. This extrapolated CaO content agrees with that measured for the small olivines in the melt (± 3-sigma of the microprobe counting statistics)

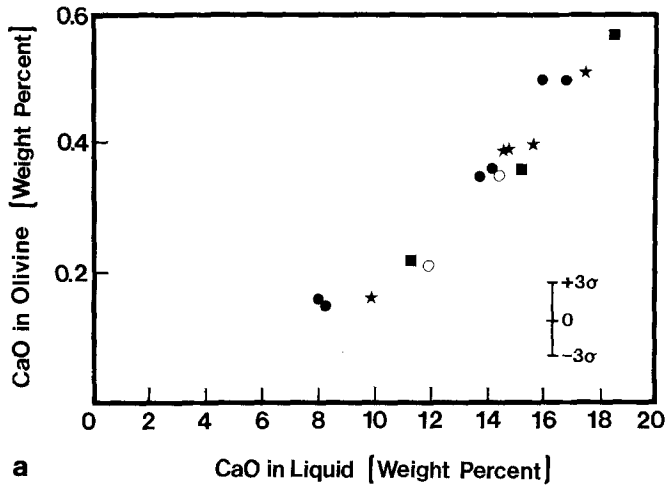

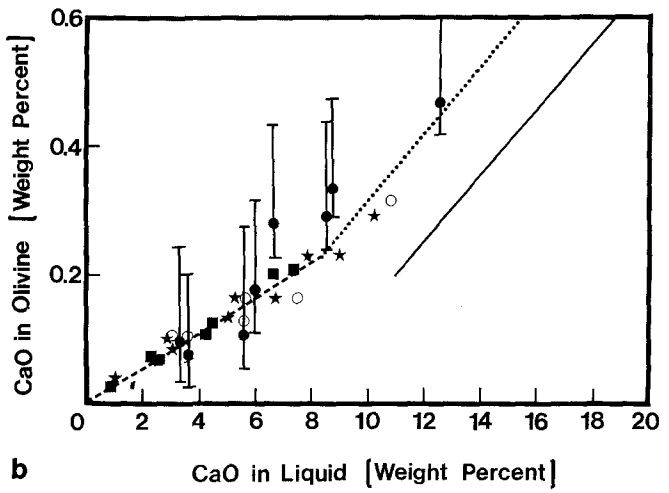

Fig. 2a, b. $CaO_{olivine}$ versus CaO_{melts}, in weight percent, for olivines having nearly equivalent compositions coexisting with a variety of melts. **a** Low-iron olivines equilibrated near one bar total pressure under a variety of temperatures and oxygen fugacities (cf. Table 2). Notice the apparent linearity in the data for melt CaO concentrations greater than 9 weight percent; the trend must change at lower CaO activities, so that it will go through the origin. Symbols: ● are runs at 1350° C, ∗ are runs at 1300° C, ■ are runs at 1250° C, and ○ are runs at 1200° C. **b** Iron-free compositions of Watson (1979). Lines: short dashes are the best-fit of Watson (1979); dotted is the hypothetical systematics at higher calcium contents; solid is the best-fit line for low-iron data in a having melts with greater than 9 weight percent CaO. Symbols: ■ are runs at 1450° C, ∗ are runs at 1350° C, ○ are runs at 1300° C, and ● are runs at 1250° C. The 1250° C data include an assumed "0.05 weight percent CaO" secondary fluorescence correction, based upon Watson's Fig. 2. This correction was substracted from the data and added back into the error bars (making them asymmetric) so that they cover the maximum probable range of calcium contents

This calculated trend does not go through the origin, however, a result inconsistent with Watson (1979).

This discrepancy can be explained by realizing that the Watson (1979) data map a predominantly low-calcium, linear regime, in which K_d is essentially independent of calcium activity. Conversely, the data from this study map a predominantly higher-calcium, non-linear regime in which K_d depends upon calcium activity (Fig. 2b). The transition between the two regimes occurs when the melts show between 10% and 12% CaO by weight in the low-iron system. Figure 2b also illustrates that there is an offset between the data the two systems. Whether this discrepancy is an artifact of the electron microprobe analysis, or is real will be discussed in the next section.

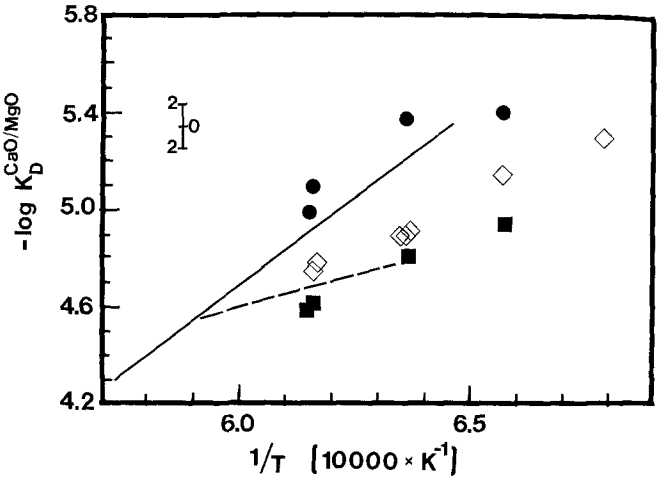

Fig. 3. $-\ln(K_D)$ versus reciprocal absolute temperature for five bulk compositions, where K_D is $(CaO/MgO)_{olivine}/(CaO/MgO)_{melt}$, the distribution coefficient is in mole percent. Symbols: ◇, △, × MMB-# 1 (~8 wt% CaO), # 2 (~13 wt% CaO) and # 3 (~16 wt% CaO), respectively (this study). Lines: dashed is the best fit for 10 kb experiments using natural NT-23 having approximately 10 weight percent CaO (Elthon and Scarfe 1984); solid is the best fit reported by Watson (1979) for the one atmosphere, iron-free data (charges having ≤16 wt% CaO)

In contrast to the calcium partitioning, the calcium/magnesium distribution is strongly temperature dependent, as shown in Fig. 3. The dependence of the molar CaO/MgO distribution coefficient. K_D, on temperature can be described by the line,

$$-\ln(K_D)=\left[\frac{(0.9\pm0.1)\,10^4}{T(\mathrm{K})}\right]-(0.8\pm0.2) \qquad (4)$$

where the errors are ±2 standard deviations of the least-squares fit. This result is consistent with the work of Watson (1979).

Visual inspection of Fig. 3 shows a small, but apparently systematic offset of each data set from "in house" experiments, corresponding to the bulk calcium concentration in each initial composition. Because the MMB-series bulk compositions differed only in CaO content, this offset probably reflects differences in CaO activity. Also in Fig. 3 are trends for similar olivines in different systems: iron-free forsterite from Watson (1979) and olivines having 87% to 90% molar forsterite, made at 10 kb from natural basalt (Elthon and Scarfe 1984).

The effect of composition

One-atmosphere experiments complementary to the low-iron (MMB-series) runs were performed to isolate the role of major element composition in calcium partitioning and distribution. These data, combined with experiments from the literature, indicate that the amount of CaO in the olivine is a strong function of the activity of iron (as Fe_2SiO_4 and FeO), as well as calcium.

Figure 4 demonstrates the effect of iron activity on calcium partitioning. In this figure, the weight-ratio calcium partition coefficient, K_d, is plotted against the molar concentra-

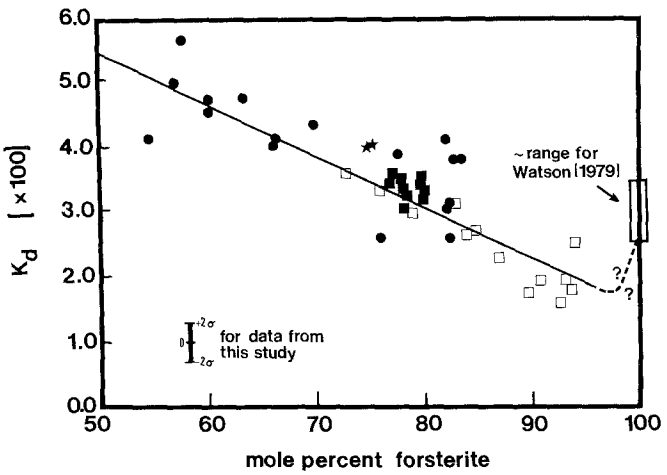

Fig. 4. The calcium partition coefficient, K_d (CaO_{olvine}/CaO_{melt}, concentrations in weight percent), versus the forsterite component of the coexisting olivine in mole percent. Data is restricted to olivine/melt pairs having melts between 8 and 15 weight percent CaO. Symbols: □ MMB-series experiments; ● iron-saturated basaltic compositions (Roeder, 1974); ● synthetic, low potassium tholeitic glass doped with excess Lu and/or Hf (Dunn 1985); * natural lunar basalts (Longhi et al. 1978); □ range of iron-free data (Watson 1979). *Solid line* is the best-fit line for the iron-bearing data. *Dashed line* indicates a probable change in partitioning behavior at very low iron concentrations (Navrotsky 1978)

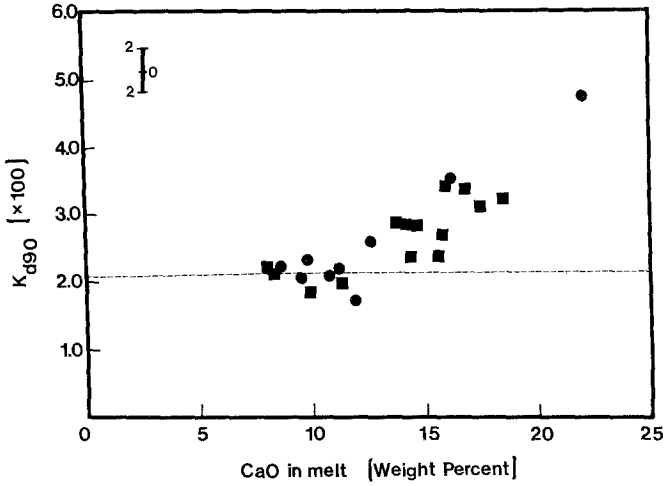

Fig. 5. The normalized weight-percent calcium partition coefficient, K_{d90}, versus calcium content of the melt for experiments from this study run near 1 bar total pressure. Data represent a several starting compositions, run under a variety of temperatures and oxygen fugacities. The bar gives an average value for the ±2-sigma error. The *dashed line* plots $K_{90}=0.021$. Symbols: ■ highly-magnesian MMB-series experiments, and ● other one-atmosphere crystallization experiments (cf Table 1)

tion of forsterite in the olivine. The trend in the data can be empirically described by the line:

$$K_d=0.01\times\{(-0.08\pm0.015)\times(\%fo)+(9.5\pm0.2)\} \quad (1)$$

where the forsterite content of the olivine, $\%fo$, is in mole percent, the errors given are 2-sigma values for the least-squares fit, and the correlation coefficient for the best fit is 0.87. The data represent a wide range of compositions, with two restrictions. First, all charges have melts with CaO concentrations between 8 and 15 weight percent, so that scatter caused by differences in calcium activity was limited. Second, all charges had molar FeO/MgO distribution coefficients between 0.28 and 0.32 (Roeder and Emslie 1970; Roeder 1974) to insure that equilibrium had been approached.

The empirical relationship given by Eq. (1) can be used to eliminate the scatter in partitioning data caused by differences in the activity of fayalite. In this study, a hypothetical olivine "standard" having 90 mole-percent forsterite was chosen for convenience. Then, all of the measured calcium partition coefficients were normalized to that of this hypothetical, standard olivine. This normalization was done by finding the expected deviation caused by the different iron activity (Eq. 1) and subtracting that from the measured partition coefficient. Accordingly, the normalized weight percent partition coefficient, K_{d90}, is related to the measured partition coefficient by the equation,

$$K_{d90}=K_d-0.0008\times(\%fo-90) \quad (2)$$

Then, to isolate influence of calcium activity, K_{d90} was plotted as a function of the weight percent calcium in the corresponding melt (Fig. 5). Data for melts with less than 11 weight-percent CaO appear consistent with a regime where there is no dependence of calcium partitioning on the concentration of CaO in he melt, having an average, normalized partition coefficient,

$$K_{d90}=0.021 \quad (3a)$$

For melts with calcium concentrations from 11% to at least 22% CaO by weight, the corrected weight-ratio partition coefficient shows a linear dependence upon the CaO content. The line which best fits this second trend is

$$K_{d90}=0.001\times\{2.2(\pm0.4)\times CaO_{melt}-4.3(\pm2.0)\} \quad (3b)$$

where the errors given are ±2-sigma and the correlation coefficient is 0.91.

Previously, in Figure 2a, CaO data for low-iron olivines were nearly linear when plotted versus the CaO in the melt. In fact, Eq. 3b implies that, for melts having greater than 11% CaO, plots of the normalized CaO in the olivine versus the CaO in the melt (weight percent), would be better approximated by a quadratic curve than a straight line.

Eq. 1 can also be used to normalize molar CaO/MgO olivine/melt distribution data. To do this, the calcium content of the olivines to that of an olivine of 90 mole percent forsterite, K_{d90} (wt% CaO) was multiplied by the concentration of calcium in the melt. This "effective" calcium content was then substituted into the original chemical analyses for the olivine and then converted to mole percent, giving CaO_{90}.

Figure 6 is a plot of the molar CaO_{90}/MgO in the olivine versus the molar CaO/MgO in the melt for all the one atmosphere experiments. Isotherms through the data were estimated visually, keeping in mind the linear nature of calcium partitioning at low calcium concentrations and the quadratic-like behavior at higher concentrations. The average error for sketching the curves through the data is estimated to be ±10° C.

To further test these CaO/MgO isotherms, data from published one-atmosphere experiments were plotted on a worksheet equivalent to Figure 6. The difference between the apparent temperature and the temperature reported for

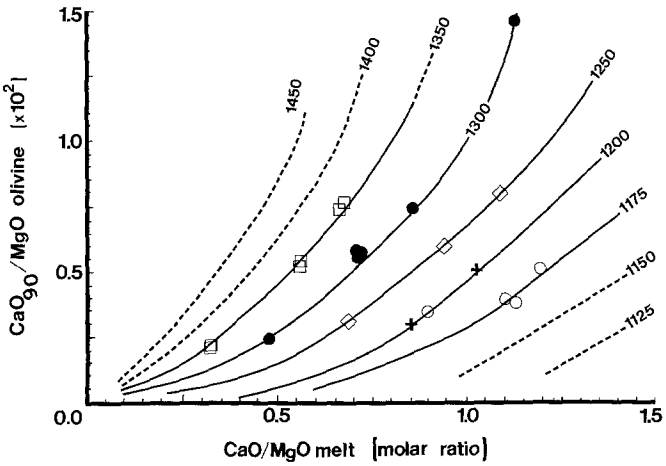

Fig. 6. Molar CaO_{90}/MgO ($\times 100$) in olivine versus molar CaO/MgO in coexisting melt, where CaO_{90} is the calcium content of an olivine standardized to reflect what it would be if the olivine was 90% forsterite. All lines are estimated: *solid lines* used data from this study; *dashed lines* are extrapolated using data from other studies. Symbols (data from this study): □ 1350° C, ● 1300° C, ◇ 1250° C, + 1220° C and ○ 1175° C

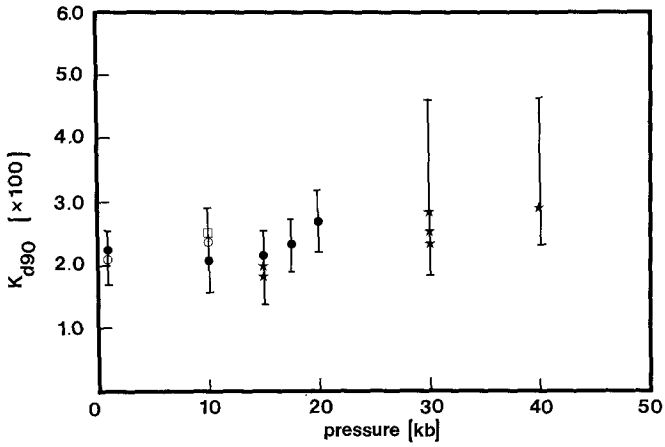

Fig. 7. The corrected calcium partition coefficient, K_{d90}, versus pressure. Symbols: ○ this study, ● synthetic, high titanium lunar basalts from (Delano 1980), re-analyzed to correct for secondary fluorescence; □ Fujii and Bougault (1983); * Brearley, Scarfe and Fujii (1984). For data from the literature, maximum values of secondary fluorescence were first estimated and then subtracted from the reported values, but were later added to the error bars

the experiment, $dT=(T_{est}-T_{act})$, was then calculated for each point. Results for 28 charges from diverse systems yielded temperature differentials, dT, of 3.3° C, with a ± 23.8° C standard deviation (Table 3).

The effect of pressure

Figure 7, is a scatter-plot of the corrected calcium partition coefficient K_{d90}, versus pressure. Included on Figure 7 are high pressure data from both this study and the literature having melt CaO contents of less than 11 wt% CaO. Note that since temperature and oxygen fugacity do not directly affect the partitioning, the correction for composition was the only correction necessary.

The error is large for these high-pressure charges. The data suggest, however, that any decrease of calcium partitioning with increasing pressure, if present, is small below 20 kb. For very high pressures (above 20 kb), the data are inconclusive.

The CaO/MgO distribution data was tested indirectly for pressure effects by plotting the deviation from the experimentally-determined isothermal lines of Figure 6. Data for terrestrial-analog systems below 20 kb show no correlation with pressure, and are given in Table 4. Because the high-pressure data was only obtained from the literature, and the low-pressure data were insufficient by themselves, no ΔV was calculated for the exchange.

Discussion

In general, the systematics for both calcium partitioning and calcium/magnesium distribution delineated by this study are consistent with findings in the current literature. For example, although previous petrologic work did not show that calcium partitioning is a strong function of melt composition, compositional variations might account for much of the scatter in the Ford et al. (1983) compiled data and might also be expected from the complexity of olivine solution models (cf. Davidson and Mukhopadhyay 1984).

There are, however, some interesting inconsistencies between the description of calcium partitioning given in this study and in Watson (1979), the analogous study of iron-free systems. Part of this descrepancy can be explained by the dependence of calcium partitioning on calcium activity: this study and Watson (1979) primarily mapped different portions of a smooth curve which bends sharply somewhere between 9% and 12% CaO by weight in the melt. Because this sharp bend does not correspond to different Si/O values of the melts (Watson 1977), nor necessarily to the onset of crystallization of another phase (cf., Table 2), it probably reflects changes in the olivine, not the melt. If so, the linear partitioning regime for lower CaO contents corresponds to Henry's Law behavior in the olivine.

The corresponding descrepancy between the description of CaO/MgO distribution systematics given in Watson (1979) and in this study can also be attributed to differences in calcium activities. Both studies did, however, find that the distribution systematics are strongly temperature dependent, in contrast to the FeO/MgO distribution coefficient (Roeder and Emslie 1970).

A less easily explained inconsistency between this study and Watson (1979) is that the data of Watson (1979) do not fit Eq. (1) of this study. This discrepancy probably does not indicate a large, systematic, analytical error, because secondary fluorescence effects were avoided and standardizations were carefully performed for both studies. If real, the discrepancy might be explained by structural differences in the corresponding iron-bearing and iron-free melts: however, the Si/O ratios of melts in the iron-free and iron-bearing systems do overlap (Watson, 1977). It is also possible that the discrepancy reflects differences in the olivines themselves: if so, generally lower calcium contents in forsterites containing minor amounts of iron may represent competition between iron and calcium for lattice sites, a "Henry's Law Problem" at low iron concentrations (Navrotsky 1978). Other workers have, however, only seen smoothly varying solution and structural properties in olivine (e.g. Brown 1982; Davidson and Mukhopadhyay 1984).

The lack of a strong pressure affect on calcium partitioning in magmatic systems is not surprising, because most predictions are based upon exchange reactions in solid systems (e.g., Warner and Luth 1973; Finnerty 1977; Adams and Bishop 1986). Evidence from the literature indicates that any pressure effect is weak below 20 kb, which encompasses many olivine-bearing magmatic systems. At 20 kb or above, the pressure may cause the CaO/MgO geothermometer to read low. Accordingly, more work needs to be done, so that a ΔV for the exchange reaction can be defined.

Petrologic applications

Because this study defined the role of composition on calcium systematics, results can be directly applied to natural systems. First, the normalized partition coefficient can be used to determine whether olivines are equilibrated with their host magmas (cf., Eqs. 3a and 3b). Then, once the existence of equilibrium has been confirmed, the CaO/MgO distribution (Figure 6) can be used as a geothermometer in magmatic systems.

Figures 8a and b illustrate how to use the normalized partition coefficient to assess equilibrium with respect to calcium between a natural olivine and its host magma. Figure 10a presents olivine tholeiites from the Loihi Seamount, Hawaii (Hawkins and Melchior, 1983). In one sample, an olivine-rich vesicular basalt, they could not use textural evidence to decide whether the olivines were chemically equilibrated with their host magma. Because the bulk composition was olivine tholeiite but the glass had very low normative olivine, the authors suspected that the rock was probably a mixture of accumulated olivine crystals and a moderately fractionated liquid. Their suspicion is supported by the fact that the olivines in this one sample do not lie on the experimental "best fit" line of the present study. The only two other anomalous points from their study are the cores of texturally-identified xenocrysts from other samples.

Figure 8b presents data from phenocrysts and xenocrysts from Baffin Bay lavas (Francis 1985). Within experimental error, all of these points lie on the "best fit" lines of this study, indicating chemical equilibrium with respect to calcium. The data set includes xenocrysts, identified by both chemical zoning and resorbed texture. This concordance among the calcium concentrations in both the phenocrysts and xenocrysts suggests two interesting possibilities: (1) that the rates of equilibration among the different cations have been different – probably an insufficient explanation, however, because calcium is thought be among the slowest cationic diffusers (Jurewicz and Watson 1988; Morioka 1981) or (2) that the calcium activity has stayed fairly constant, while that of other major components may have changed.

For samples equilibrated with respect to calcium and magnesium, normalized data can be plotted on Figure 6 for geothermometry. This was done for the published olivine/melt analyses given Leeman and Scheidegger (1977) so that the CaO/MgO exchange could be compared with other geothermometers (Table 5). Temperatures estimated using the CaO/MgO equilibrium compare favorably with the average of the published temperatures.

We estimate the sensitivity of the geothermometer to be about 25° C (1 sigma) for quenched low-pressure glasses (the sensitivity estimate was made by calculating CaO/MgO

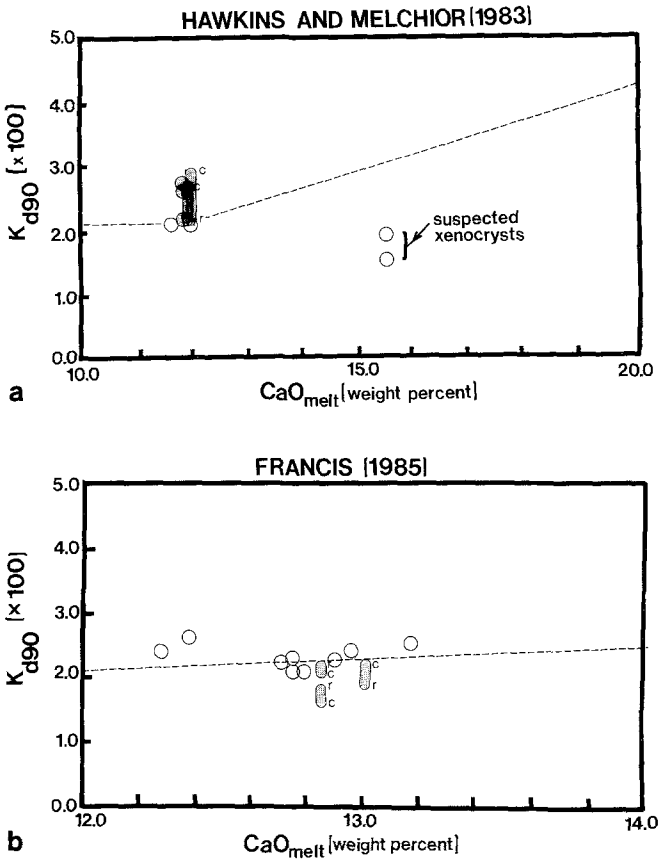

Fig. 8a, b. Using K_{90} versus the CaO concentration of the melt as a test for calcium equilibrium in natural samples. Dashed lines are from Eqs. 3a and 3b. Symbols: *Open circles* are texturally-determined phenocrysts, *shaded circles* are texturally-determined xenocrysts, and *shaded bars* are the range of standardized calcium partition coefficient found for the rims, r, and cores, c, of zoned olivines; **a** Data from Hawkins and Melchior (1983), where points marked "suspected xenocrysts" are from a sample suspected to have accumulated excess olivine (see text); **b** Data from Francis (1985), in which, whithin the experimental uncertainty, all points – even the zoned olivines – can be considered equilibrated with respect to calcium with the host magma

temperatures for 28 one-atmosphere experiments compiled from the literature: the mean difference between the actual temperature and the estimated temperature was 3.3° C, and the standard deviation was ±23.8° C; cf., Table 3). Closure temperatures are estimated in Jurewicz and Watson (1988). This geothermometer has not been calibrated for high pressures (20 kb and above). Accordingly, care must be taken when doing geothermometry on specimens which may have been equilibrated at high pressure.

In principle, if the calcium and magnesium contents of the olivine can independently be shown to be equilibrated with the host magma, consistently low calcium/magnesium distribution temperatures may indicate that the olivine was crystallized at pressures above 15 kb. With this possibility in mind, Figure 6 was used to determine temperatures of olivine crystallization for the Baffin Bay lavas (Francis 1985; Figure 10b). For comparison, temperatures were also calculated for the two data sets using both magnesium and manganese partitioning (Leeman and Scheidegger 1977) while Francis (1985) provided independent temperature estimates based upon the cation equilibria of Ford et al. (1983) and Hart and Davis (1978). The temperatures esti-

mated for the Francis (1985) data using the CaO/MgO equilibrium are consistently low (Table 6). While the data may reflect problems with closure of olivines with respect to Mg diffusion, consistently low temperatures may also indicate that the olivines in the picrite coexisted with the melt at moderately high pressures.

Conclusions

The calcium contents of most equilibrated natural magmatic olivines reflect the melt composition. Low calcium contents in olivines can be caused by either low iron content and/or low calcium concentrations in the melt. Oxygen fugacity has no direct effect. Temperature influences the CaO/MgO distribution, but does not directly affect calcium partitioning. Pressure has a negligible effect in magmatic systems below 20 kb, but further experiments are needed to constrain the role of high pressures in calcium olivine/melt systematics.

Acknowledgements. This research benefited from both technical support and constructive criticism from a number of people, most notably: K.E. Davis, J.W. Delano, T.M. Harrison, H.B. Hollinger, and S.R. Jurewicz. The work was supported by the Division of Earth Sciences of the National Science Foundation, under grant no. EAR84-06200.

References

Adams GE, Bishop FC (1986) The olivine-clinopyroxene geobarometer: experimental results in the CaO-FeO-MgO-SiO_2 system. Contrib Mineral Petrol 94:230–237

Arculus RJ, Delano JW (1981) Intrinsic oxygen fugacity measurements: techniques and results for spinels from upper mantle peridotites and megacryst assemblages. Geochem Cosmochim Acta 45:899–913

Bickle MJ, Ford CE, Nisbit EG (1977) The petrogenesis of peridotitic komatiites: evidence from high-pressure melting experiments. Earth Planet Sci Lett 37:97–106

Biggar GM, O'Hara MJ (1969) Monticellite and forsterite crystalline solution: J Amer Cer Soc 52:249–252

Brearley M, Scarfe CM, Fujii T (1984) The petrology of ultramafic xenoliths from Summit Lake, near Prince George, British Columbia. Contrib Mineral Petrol 88:53–63

Brown GE (1982) Olivines and Silicate Spinels. In: Ribbe PH (ed) Orthosilicates, Vol 5. Reviews in Mineralogy. Mineral Soc Am, USA 275–365

Crank J (1975) The Mathematics of Diffusion, 2nd ed. Oxford University Press, London, 414 pp

Darken LS, Gurry RW (1945) The system iron-oxygen. I. The wustite field and related equilibria. J Amer Chem Soc 68:1398–1412

Davidson PM, Mukhopadhyay DK (1984) Ca–Fe–Mg olivines: phase relations and a solution model. Contrib Mineral Petrol 86:256–263

Deines P, Nafziger RH, Ulmer GC, Woermann E (1974) Temperature-oxygen fugacity tables for selected gas mixtures in the system C–H–O at one atmosphere total pressure. Earth Mineral Sci Exper Sta, Bull, The Penn State Univ College of Earth and Mineral Sci 88:129p

Delano JW (1980) Chemistry and liquidus phase relations of Apollo 15 red glass: implications for the deep lunar interior. Proc Lunar Planet Sci Conf 11th, pp 251–288

Dunn T (1987) Partitioning of Hf, Lu, Ti, and Mn between olivine, clinopyroxene and basaltic liquid. Contrib Mineral Petrol 96:476–484

Elthon D, Scarfe CM (1984) High-pressure phase equilibria of a high-magnesia basalt and the genesis of primary oceanic basalts. Amer Mineral 69:1–15

Finnerty TA (1977) Exchange of Mn, Ca, Mg, and Al between synthetic garnet, orthopyroxene, clinopyroxene, and olivine. Carnegie Inst Wash Year Bk 76:572–579

Ford CE, Russel DG, Craven JA, Fisk MF (1983) Olivine-liquid equilibria: temperature, pressure and composition dependence of the crystal/liquid cation partition coefficients for Mg, Fe^{+2}, Ca, and Mn. J Petrol 24:256–265

Francis D (1985) The Baffin Bay lavas and the value of picrites as analogous of primary magmas. Contrib Mineral Petrol 89:144–154

Fujii T, Bougault H (1983) Melting relations of a magnesian abyssal tholeiite and the origin of MORB's. Earth Planet Sci Lett 62:283–295

Ford CE, Russell DG, Craven JA, Fisk MR (1983) Olivine-liquid equilibria: temperature, pressure and composition dependence of the crystal/liquid cation partition coefficients for Mg, Fe^{+2}, Ca and Mn. J Petrol 24:256–265

Goldstein JI, Yakowitz H, Newburg DE, Lifshin E, Colby JW, Coleman JR (1975) Practical Scanning Electron Microscopy: Plenum Press, New York 582 p

Harrison TM, Watson EB (1983) Kinetics of zircon dissolution and zirconium diffusion in granitic melts of variable water content. Contrib Mineral Petrol 84:66–72

Hawkins J, Melchior J (1983) Petrology of basalts from Loihi Seamount, Hawaii. Earth Planet Sci Lett 66:356–368

Huebner SJ (1971) Buffering techniques for hydrostatic systems at elevated pressures. In: Ulmer GC (ed) Research Techniques for High Pressure and High Temperature. Springer, New York Berlin Heidelberg, pp 123–177

Jurewicz, AJG (1986) Effect of temperature, pressure, oxygen fugacity and composition on calcium partitioning, calcium-magnesium distribution and the kinetics of cation exchange between olivines and basaltic melts. Ph D thesis, Rensselaer Polytech Inst, 216 pp

Jurewicz AJG, Watson EB (1988) Cations in Olivines, Part 2: Diffusion in olivine xenocrysts, with applications to petrology and mineral physics. Contrib Mineral Petrol 99:186–201

Leeman WP, Scheidegger KF (1977) Olivine/liquid distribution coefficients and a test for crystal-liquid equilibrium. Earth Planet Sci Lett 35:247–257

Longhi J, Walker D, Hays JF (1978) The distribution of Fe and Mg between olivine and lunar basaltic liquids. Geochim Cosmochim Acta 42:1545–1558

Misener DJ (1974) Cationic diffusion in olivine to 1400° C and 35 kbar. In: Hofmann AW, Giletti BJ, Yoder HS, Jr, Yund RA (eds) Geochemical Transport and Kinetics. pp 117–129, Carnegie Inst of Washington, 634 p

Morioka M (1981) Cation diffusion in olivine – II. Ni–Mg, Mn–Mg, Mg and Ca. Geochim Cosmochim Acta 45:1573–1580

Murata KJ, Bastron H, Brannock WW (1965) X-ray determinative curve for Hawaiian olivines of composition Fo_{76-88}. US Geol Survey Prof Paper 525-C:35–37

Navrotsky A (1978) Thermodynamics of element partitioning: (1) Systematics of transition metals in crystalline and molten silicates and (2) Defect chemistry and the "Henry's Law Problem". Geochem Cosmochim Acta 42:887–902

Nitsan U (1974) Stability field of olivine with respect to oxidation and reduction. J Geophys Res 79:706–711

Roeder PL (1974) Activity of iron and olivine solubility in basaltic liquids. Earth Planet Sci Lett 23:397–410

Roeder PL, Emslie RF (1970) Olivine-liquid equilibrium. Contrib Mineral Petrol 29:275–289

Sahama ThG, Hytonen K (1958) Calcium-bearing magnesium-iron olivines. Amer Mineral 43:862–871

Sato M (1971) Electrochemical measurements and control of oxygen fugacity and other gaseous fugacities with solid electrolyte sensors. In: Ulmer GC (ed) Research Techniques for High Pressure and High Temperature. Springer, New York Berlin Heidelberg, pp 43–99

Simkin T, Smith JV (1970) Minor-element distribution in olivine. J Geol 78:304–325

Stolper E (1980) A phase diagram for mid-ocean ridge basalts: preliminary results and implications for petrogenesis. Contrib Mineral Petrol 74:13–27

Stormer JC (1973) Calcium zoning in olivine and its relationship to silica activity and pressure. Geochim Cosmochim Acta 37:1815–1821

Walker D, Shibata T, DeLong SE (1979) Abyssal tholeiites from the Oceanographer Fracture Zone: II. Phase equilibria and mixing. Contrib Mineral Petrol 70:111–125

Warner RD, Luth WC (1973) Two-phase data for the join monticellite ($CaMgSiO_4$)-forsterite (Mg_2SiO_4): experimental results and numerical analysis. Amer Mineral 58:998–1008

Watson EB (1977) Partitioning of manganese between forsterite and silicate liquid. Geochim Cosmochim Acta 41:1363–1374

Watson EB (1979) Calcium content of forsterite coexisting with silicate liquid in the system $Na_2O-CaO-MgO-Al_2O_3-SiO_2$. Amer Mineral 64:824–829

Watson EB, Green TH (1981) Apatite/liquid partition coefficients for the rare earth elements and strontium. Earth Planet Sci Lett 56:405–421

Watson EB, Harrison TM, Ryerson FJ (1985) Diffusion of Sm, Sr, and Pb in fluorapatite. Geochim Cosmochim Acta 49:1813–1823

Yang H-Y (1973) New data on forsterite and monticellite solid solutions. Amer Mineral 58:343–345

Received December 23, 1986 / Accepted March 3, 1988
Editorial responsibility: I.S.E. Carmichael